

Jahn-Teller Stabilization Energies for f^x Systems: Angular-Overlap Calculations for Octahedral Systems in the Weak-Field Scheme

KEITH D. WARREN

Received November 17, 1981

The angular-overlap model previously used for the calculation of the linear Jahn-Teller coupling constants for MX_6 , O_h , f^1 systems in the strong-field scheme is extended to treat f^x species ($x = 1-3$) in the more convenient weak-field, $|\text{LSJM}_J\rangle$, basis. Results are given in general form for the Jahn-Teller-active components of the ${}^2F_{5/2}$ and ${}^2F_{7/2}$ states of f^1 and for the similarly active components of the 3H_4 and ${}^4I_{9/2}$ states of f^2 and f^3 , respectively. Possible manifestations of Jahn-Teller activity for the excited states of the f^2 , 3H_4 , manifold and for the ground and excited states of the f^3 , ${}^4I_{9/2}$, manifold are discussed in the light of the available experimental data for the appropriate lanthanide and actinide species.

Introduction

Recently it was demonstrated by Bacci¹ that the angular-overlap model could be adapted for the calculation of the linear Jahn-Teller coupling constants in terms of quantities involving only the standard angular-overlap parameters (e_λ) and the internuclear distance (R), or their derivatives ($\partial e_\lambda/\partial R$), and this technique was extended by the author² to treat f -orbital degeneracies for MX_6 , O_h , species. Since the main objective of this latter work was merely to ascertain the probable magnitude of Jahn-Teller effects involving f -orbital degeneracies, attention was largely focused simply on f^1 species, and, because both the angular-overlap parameters and the Jahn-Teller coupling constants are most easily evaluated in the strong-field scheme, this basis set was adopted for all the calculations, although the effects of spin-orbit coupling were also specifically included.

However, the electronic states arising for f^x species of the lanthanide series are much better described in terms of the weak-field, $|\text{LSJM}_J\rangle$, scheme, and even for actinide systems this basis set constitutes the preferred mode of description. Moreover, as the number of f electrons in the f^x shell increases, the strong-field model becomes progressively more unrealistic, and any meaningful attempt to treat, for example, f^2 and f^3 systems—the latter affording, in octahedral symmetry, the possibility of a Jahn-Teller-active ground level—must of necessity utilize the weak-field scheme.

In this work therefore all the nonvanishing one-electron matrix elements of the angular-overlap model are first evaluated in the strong-field basis: these are then converted to the weak-field $|m_l\rangle$ basis and finally used in conjunction with the symmetry-adapted O^* weak-field $|\text{LSJM}_J\rangle$ functions for f^1 , f^2 , and f^3 configurations in order to calculate the linear Jahn-Teller coupling constants (and the Jahn-Teller stabilization energies, E_{JT}) for the active components of the appropriate ground-state manifolds. Since the data for f^1 systems have already been discussed,² attention is here concentrated on possible Jahn-Teller effects in the excited states of the f^2 , 3H_4 , manifold, and on the f^3 , ${}^4I_{9/2}$, system for which, in O^* , a Jahn-Teller-active, Γ_8 , ground component is likely to arise.

Theory

The basic theory of the calculation of the linear Jahn-Teller coupling constants via the angular-overlap model has been given previously,^{1,2} and reference should be made thereto for further details. The coupling constant, c , is defined as

$$c = \langle \psi_a | \partial V / \partial Q^\Gamma_\gamma | \psi_b \rangle$$

where Q^Γ_γ is the Jahn-Teller-active normal coordinate, being

the component, γ , of the Γ representation. Combining this with the standard form for the angular-overlap matrix element yields

$$c = \sum_\lambda \sum_{j=1}^N \frac{\partial [e_{\lambda\omega} F^l_{\lambda\omega}(\psi_a) F^l_{\lambda\omega}(\psi_b)]}{\partial (R_j, \theta_j, \varphi_j)} \frac{\partial (R_j, \theta_j, \varphi_j)}{\partial Q^\Gamma_\gamma}$$

from which the appropriate coupling constants are readily derived. Here the $F^l_{\lambda\omega}$ are the elements of the general angular transformation matrix, θ_j and φ_j are the polar angles defining the positions of the j th of the N ligands, and the $e_{\lambda\omega}$ are the standard angular-overlap parameters. For Jahn-Teller-active vibrations representing stretching modes the c quantities will be functions of $\partial e_\lambda/\partial R$, but for those corresponding to bending modes the c terms will involve simply e_λ/R . For O_h MX_6 systems these active vibrational modes are the ϵ_g (stretching) and τ_{2g} (bending) vibrations, of which the former may couple with either E or T degeneracies, but the latter only with T states.

For such an O_h MX_6 system the real f -orbital set will transform as $a_{2u} + t_{1u} + t_{2u}$, and if only s and p orbitals of the ligands are considered (and δ and φ bonding as usual neglected), the a_{2u} level will be nonbonding, the t_{2u} level π antibonding, and the t_{1u} level both σ and π antibonding, so that both e_σ and e_π terms must be included in the calculation. Thus, in the earlier treatment of f -orbital Jahn-Teller effects² the strong-field basis set of the real orbitals, f_{z^2} , $f_{x^2-y^2}$, f_{yz} , $f_{x(x^2-3y^2)}$, and $f_{y(3x^2-y^2)}$, was employed, although it only proved necessary to evaluate certain matrix elements within the related cubic basis sets, f_{x^3} , f_{y^3} , and f_{z^3} (t_{1u}) and $f_{x(x^2-y^2)}$, $f_{x(x^2-y^2)}$, and $f_{y(x^2-x^2)}$ (t_{2u}). In this way the appropriate Jahn-Teller stabilization energies were calculated for the f^1 states, ${}^2T_{1u}(t_{1u})$ and ${}^2T_{2u}(t_{2u})$, and it was simple to derive therefrom the corresponding E_{JT} values for the active Γ_8 levels generated when spin-orbit coupling is included.

However, the coupling constants thus derived² for the f^1 system strictly apply only to pure strong-field states, and these will be substantially mixed by the appreciable spin-orbit coupling. Moreover, even though the more realistic and purer f^1 weak-field states may be expressed in terms of their strong-field counterparts by use of the spin-orbit matrices and eigenfunctions given by Eisenstein and Pryce,³ the resulting calculation properly requires a number of cross-product matrix elements not previously listed, and it is therefore much simpler first to calculate *all* the nonzero Jahn-Teller matrix elements of e_σ and e_π (and their derivatives) in the original real-orbital strong-field basis and then to convert them to the corresponding weak-field quantities in the $|m_l\rangle$ basis. (See the supplementary material.) Finally, for completion of the

(1) M. Bacci, *Chem. Phys. Lett.*, **58**, 537 (1978).(2) K. D. Warren, *Inorg. Chem.*, **19**, 653 (1980).(3) J. C. Eisenstein and M. H. L. Pryce, *Proc. R. Soc. London, Ser. A*, **255**, 181 (1960).

Table I. Jahn-Teller Coupling Constants for f^1 Systems in the Strong- and Weak-Field Schemes^{a,c}

Strong-Field Scheme			
Trigonal Coupling			
$\Gamma_8(^2T_{1u}) \otimes \tau_{2g}$	$A\tau = -3^{1/2}(\sigma - \pi)$		$E_{JT} = A\tau^2/2K_\tau$
$\Gamma_6(^2T_{2u}) \otimes \tau_{2g}$	$A\tau = -(5/6)(3^{1/2})\pi$		
Tetragonal Coupling			
$\Gamma_8(^2T_{1u}) \otimes \epsilon_g$	$A\epsilon = -3^{1/2}[(1/3)\dot{\sigma} - (1/8)\dot{\pi}]$		$E_{JT} = A\epsilon^2/2K_\epsilon$
$\Gamma_8(^2T_{2u}) \otimes \epsilon_g$	$A\epsilon = (5/24)(3^{1/2})\dot{\pi}$		
Weak-Field Scheme			
Trigonal Coupling			
$\Gamma_8(^2F_{5/2}) \otimes \tau_{2g}$	$A\tau = -3^{1/2}[(2/7)\sigma + (4/21)\pi]$		$E_{JT} = A\tau^2/2K_\tau$
$\Gamma_8(^2F_{7/2}) \otimes \tau_{2g}$	$A\tau = -5(3^{1/2})[(1/7)\sigma - (1/14)\pi]$		
Tetragonal Coupling			
$\Gamma_8(^2F_{5/2}) \otimes \epsilon_g$	$A\epsilon = 3^{1/2}[(3/14)\dot{\sigma} + (11/42)\dot{\pi}]$		$E_{JT} = A\epsilon^2/2K_\epsilon$
$\Gamma_8(^2F_{7/2}) \otimes \epsilon_g$	$A\epsilon = 5(3^{1/2})[(1/42)\dot{\sigma} - (1/28)\dot{\pi}]$		

^a The K_ϵ and K_τ parameters are respectively the force constants for the ϵ_g and τ_{2g} vibrational modes. ^b For the case $\Gamma_8 \otimes \epsilon_g$ the coupling constant, $A\epsilon$, is $1/2$ times the value of the constant, C , for the parent $T_{1,2}$ level, where $E_{JT}(T_{1,2}) = C^2/2K_\epsilon$; for $\Gamma_8 \otimes \tau_{2g}$ the coupling constant, $A\tau$, is $1/3^{1/2}$ times the value of the constant, B , for the parent $T_{1,2}$ level, where $E_{JT}(T_{1,2}) = 2B^2/3K_\tau$. Since, for either coupling, $E_{JT}(\Gamma_8) = A\Gamma^2/2K\Gamma$, it follows that in both cases $E_{JT}(\Gamma_8) = 1/4E_{JT}(T_{1,2})$. See Bersuker⁸ for definitions of the constants B and C . See also Liehr⁷ for discussion of the Γ_8 Jahn-Teller matrix, which takes the form, following the conventions of Bersuker

$$\begin{vmatrix} \Gamma_8^1 & & & \\ & \Gamma_8^2 & & \\ & & \Gamma_8^3 & \\ & & & \Gamma_8^4 \end{vmatrix} \begin{vmatrix} A_\epsilon(Q_{zz}^2) - \epsilon' & 0 & A_\epsilon(Q_{xx}^2 - y^2) - A_\tau(Q_{xx} + iQ_{yz}) & \\ 0 & A_\epsilon(Q_{zz}^2) - \epsilon' & A_\tau(Q_{xx} - iQ_{yz}) - A_\epsilon(Q_{xx}^2 - y^2) & \\ A_\epsilon(Q_{xx}^2 - y^2) + A_\tau(iQ_{xy}) & A_\tau(Q_{xx} + iQ_{yz}) & -A_\epsilon(Q_{zz}^2) - \epsilon' & 0 \\ A_\tau(Q_{xx} - iQ_{yz}) & A_\tau(iQ_{xy}) - A_\epsilon(Q_{xx}^2 - y^2) & 0 & -A_\epsilon(Q_{zz}^2) - \epsilon' \end{vmatrix} = 0$$

Solving $\Gamma_8 \otimes \epsilon_g$ and $\Gamma_8 \otimes \tau_{2g}$ separately then yields $E_{JT}(\epsilon_g) = A\epsilon^2/2K_\epsilon$, and $E_{JT}(\tau_{2g}) = A\tau^2/2K_\tau$. ^c Here and throughout $\sigma = e_{O/R}$, $\pi = e_{\pi/R}$, $\dot{\sigma} = \partial e_{O/R}/\partial R$, and $\dot{\pi} = \partial e_{\pi/R}/\partial R$.

calculation in the weak-field scheme the corresponding $|LSJM_J\rangle$ wave functions are required together with the symmetry-adapted O^* linear combinations of the various $|M_J\rangle$ components. The latter have been given for the f^1 system by Reisfeld and Crosby,⁴ and by Satten and Margolis⁵ for the 3H_4 state of f^2 , while Lea, Leask, and Wolf⁶ have listed the required eigenfunctions for the $^4I_{9/2}$ state of f^3 and for other f^2 systems. The desired Jahn-Teller coupling constants may thus be readily derived in the weak-field basis once the appropriate $|LSJM_J\rangle$ matrix elements have been expressed in terms of the $|m_l\rangle$ quantities.

As an illustration (see Figure 1) the f^1 system may be considered. When spin-orbit effects are explicitly included, the strong-field states $^2T_{1u}(t_{1u})$ and $^2T_{2u}(t_{2u})$ yield respectively $\Gamma_6 + \Gamma_8$ and $\Gamma_7 + \Gamma_8$ levels. The Γ_6 and Γ_7 Kramers doublets are both Jahn-Teller impotent, and the activity of the threefold ($t_{1,2}$) orbital degeneracy is partially quenched and restricted to the components of Γ_8 symmetry. Such a Γ_8 level, arising from a T orbital state, may couple⁷ with either the ϵ_g or the τ_{2g} vibrational mode, and in both cases E_{JT} is reduced to one-fourth of its former value.

In the alternative weak-field scheme it is similarly found that the states $^2F_{5/2}$ and $^2F_{7/2}$ yield respectively $\Gamma_7 + \Gamma_8$ and

Table II. Jahn-Teller Coupling Constants for f^2 , 3H_4 , Systems in the Weak-Field Scheme^{a,b}

Trigonal Coupling			
$\Gamma_4 T_1(^3H_4) \otimes \tau_{2g}$	$B = (12/55)\sigma + (3/5)\pi$		$E_{JT} = 2B^2/3K_\tau$
$\Gamma_5 T_2(^3H_4) \otimes \tau_{2g}$	$B = (676/385)\sigma - (701/385)\pi$		
Tetragonal Coupling			
$\Gamma_3 E(^3H_4) \otimes \epsilon_g$	$A = 3^{1/2}[(88/315)\dot{\sigma} - (76/1155)\dot{\pi}]$		$E_{JT} = A^2/2K_\epsilon$
$\Gamma_4 T_1(^3H_4) \otimes \epsilon_g$	$C = -3^{1/2}[(109/495)\dot{\sigma} + (62/165)\dot{\pi}]$		
$\Gamma_5 T_2(^3H_4) \otimes \epsilon_g$	$C = 3^{1/2}[(863/3465)\dot{\sigma} - (26/105)\dot{\pi}]$		$E_{JT} = C^2/2K_\epsilon$

^a In O^* 3H_4 yields Γ_1 (inactive) + $\Gamma_3 + \Gamma_4 + \Gamma_5$. ^b The $E \otimes \epsilon_g$ Jahn-Teller matrix takes the form given by Bersuker,⁸ but that for $T_{1,2} \otimes (\epsilon_g + \tau_{2g})$, although entirely equivalent to the result there given, takes the form

$$\begin{vmatrix} T_{1,2} \otimes (\epsilon_g + \tau_{2g}) & & & \\ & T_{1,2}^a & & \\ & & T_{1,2}^b & \\ & & & T_{1,2}^c \end{vmatrix} \begin{vmatrix} C(Q_{zz}^2) - \epsilon' & 2^{1/2}B(Q_{xz} - iQ_{yz}) & 2^{1/2}B(Q_{xz} + iQ_{yz}) \\ 2^{1/2}B(Q_{xz} + iQ_{yz}) & -1/2C(Q_{zz}^2) - \epsilon' & B(iQ_{xy}) + (1/2)3^{1/2}C(Q_{xx}^2 - y^2) \\ 2^{1/2}B(Q_{xz} - iQ_{yz}) & -B(iQ_{xy}) + (1/2)3^{1/2}C(Q_{xx}^2 - y^2) & -1/2C(Q_{zz}^2) - \epsilon' \end{vmatrix} = 0$$

Solving $T_{1,2} \otimes \epsilon_g$ and $T_{1,2} \otimes \tau_{2g}$ separately yields, as before, $E_{JT}(\epsilon_g) = C^2/2K_\epsilon$; $E_{JT}(\tau_{2g}) = 2B^2/3K_\tau$.

$\Gamma_6 + \Gamma_7 + \Gamma_8$ in O^* symmetry, and the coupling constants calculated for the active Γ_8 levels are given in Table I together with the strong-field results for comparison. In the strong-field scheme the coupling constants for the t_{1u} degeneracies contain both e_σ and e_π terms, while those for t_{2u} degeneracies involve only e_π , but the constants for the Γ_8 levels of the weak-field states, $^2F_{5/2}$ and $^2F_{7/2}$, all contain both e_σ and e_π contributions; for a given coupling, the sum of the coupling constants over the whole f^1 manifold is invariant between the weak- and strong-field bases.

However, the determination of the Jahn-Teller coupling constants for the $^2F_{5/2}$ and $^2F_{7/2}$ states requires the intermediate evaluation of matrix elements between various M_J components of the form $\langle M_J | \partial V / \partial Q_\gamma^\Gamma | M_J' \rangle$, and for the several $\partial V / \partial Q_\gamma^\Gamma$ operators (hereinafter abbreviated to Q_γ) the relevant nonzero terms are listed in the supplementary material. For the f^1 system the $|M_J\rangle$ components and the O^* $|LSJM_J\rangle$ functions are both relatively simple expressions, and it is therefore easy to find all the matrix elements within the Γ_8 states, to check that these follow the general form given by Liehr⁷ and to derive the coupling constants therefrom. For the f^2 , 3H_4 , state all the nonzero matrix elements needed are again given in the supplementary material and the derived coupling constants in Table II, the forms of the Jahn-Teller matrix elements within the E, T_1 , and T_2 manifolds all being the same as, or equivalent to, those of Liehr⁷ and Bersuker.⁸ Here the 3H_4 ground level in O^* yields the components Γ_1 (A_1), Γ_3 (E), Γ_4 (T_1), and Γ_5 (T_2), the first of these being inactive while the Γ_3 (E) level may couple with ϵ_g , and the Γ_4 (T_1) and Γ_5 (T_2) levels with both ϵ_g and τ_{2g} . Here however the $|M_J\rangle$ components are much more complicated functions than for f^1 , and the calculation of the Q_γ matrix elements is correspondingly more tedious. For the $^4I_{9/2}$ state of f^3 the situation is worse and further complicated by the fact that in O^* $^4I_{9/2}$ yields an inactive Γ_6 level and two active Γ_8 components. Consequently, the appropriate symmetry-adapted O^* functions cannot be written in closed form (as linear combinations of various $|M_J\rangle$ contributions) since the relevant eigenvectors depend upon the ratio of the fourth- and sixth-degree terms in the octahedral potential, although numerical solutions have been presented

- (4) M. J. Reisfeld and G. A. Crosby, *Inorg. Chem.*, **4**, 65 (1965).
 (5) R. A. Satten and J. S. Margolis, *J. Chem. Phys.*, **32**, 573 (1960).
 (6) K. R. Lea, M. J. M. Leask, and W. P. Wolf, *J. Phys. Chem. Solids*, **23**, 1381 (1962).
 (7) A. D. Liehr, *J. Phys. Chem.*, **67**, 389 (1963).

- (8) I. B. Bersuker, *Coord. Chem. Rev.*, **14**, 357 (1975).

Table III. Jahn-Teller Coupling Constants for $f^3, {}^4I_{9/2}$, Systems in the Weak-Field Scheme^a

$\Gamma_8^{(1)} \otimes \epsilon_g$		$\Gamma_8^{(1)} \otimes \tau_{2g}$		$\Gamma_8^{(2)} \otimes \epsilon_g$		$\Gamma_8^{(2)} \otimes \tau_{2g}$		x	B_0^6/B_0^4	e_π/e_σ
σ	π	σ	π	σ	π	σ	π			
-0.3474	+0.5843	-1.2524	+2.1312	-0.0564	+0.3805	+0.4283	-0.7568	0.00	∞	-3.0000
-0.3543	+0.5921	-1.3422	+2.2848	-0.0495	+0.3726	+0.5181	-0.9104	0.20	+1.0218	-0.8849
-0.3606	+0.6000	-1.4367	+2.4465	-0.0431	+0.3646	+0.6127	-1.0723	0.40	+0.3832	-0.1244
-0.3655	+0.6074	-1.5299	+2.6059	-0.0383	+0.3574	+0.7058	-1.2316	0.60	+0.1703	+0.2672
-0.3674	+0.6125	-1.6113	+2.7452	-0.0363	+0.3518	+0.7874	-1.3710	0.80	+0.0639	+0.5059
-0.3654	+0.6157	-1.6696	+2.8444	-0.0384	+0.3490	+0.8455	-1.4701	1.00	0.0000	+0.6667

^a The table lists the values of the Jahn-Teller coupling constants A_ϵ and A_τ , where for both couplings $E_{JT} = A\Gamma^2/2K\Gamma$. In O^* symmetry ${}^4I_{9/2} = \Gamma_6 + \Gamma_8^{(1)} + \Gamma_8^{(2)}$, and for f^3 systems $\Gamma_8^{(2)}$ will usually constitute the ground component and $\Gamma_8^{(1)}$ a higher lying excited state. The nomenclature follows that of Lea, Leask, and Wolf,⁶ and the parameter, x , which represents the ratio of the fourth- and sixth-degree terms in the octahedral potential, is as therein defined. The last two columns give the ratio of the crystal field parameters, B_0^4/B_0^6 (see ref 2) and of the angular-overlap parameters, e_π/e_σ .

by Lea, Leask, and Wolf.⁶ The $f^3, {}^4I_{9/2}$, problem can therefore be tackled as usual via the calculation of the relevant $\langle M_j | Q_\gamma | M_j' \rangle$, but it is fortunately unnecessary to evaluate all the different Q_γ terms since the effort involved may be minimized and an internal check applied to the results via an operator technique that utilizes the equivalents listed by Hutchings.⁹

Thus, because nonzero matrix elements of the Jahn-Teller operators $Q_{x^2-y^2}$ and Q_{xy} occur as off-diagonal terms in the couplings of the ϵ_g mode to E, T_1, T_2 , and Γ_8 states, or of the τ_{2g} mode to T_1, T_2 , and Γ_8 states (and from these the appropriate coupling constants can be easily derived), it is unnecessary also to evaluate the matrix elements of the operators Q_{z^2}, Q_{xz} , and Q_{yz} . Moreover, for an f-orbital basis set, the octahedral potential may be written in the operator-equivalent form as

$$V_{\text{oct}} = b[O_4^0 + 5O_4^4] + c[O_6^0 - 21O_6^4]$$

where b and c are multiplicative factors and the O_n^m are Stevens¹⁰ type operator equivalents. The vibrational mode, $Q_{x^2-y^2}$, may similarly be expressed as an operator equivalent, $a'O_2^2$, and since the mode Q_{xy} corresponds to an operator of similar order and degree, it is clear that the Jahn-Teller operators $\partial V/\partial Q_{x^2-y^2}$ and $\partial V/\partial Q_{xy}$ may also be expressed in terms of operator equivalents and will contain only terms in O_2^2, O_4^2, O_6^2 , and O_6^6 . From the various $\langle M_j | \partial V/\partial Q | M_j' \rangle$ terms already evaluated for the ${}^2F_{5/2}, {}^2F_{7/2}$, and 3H_4 states it is readily shown that the Jahn-Teller operators may be written as

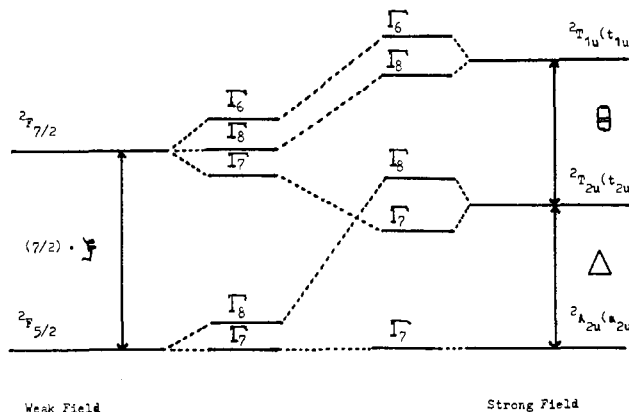
$$\partial V_{\text{oct}}/\partial Q_{x^2-y^2} = \alpha'O_2^2 + \beta'O_4^2 + \gamma'(5O_6^2 + 11O_6^6)$$

and

$$\partial V_{\text{oct}}/\partial Q_{xy} = \alpha''O_2^2 + \beta''O_4^2 + \gamma''(5O_6^2 + 33O_6^6)$$

where the matrix elements of $Q_{x^2-y^2}$ are in units of $\partial e_\sigma/\partial R$ or $\partial e_\pi/\partial R$ and those of Q_{xy} in units of ie_σ/R or ie_π/R , different α, β , and γ values obtaining for the σ and π contributions.

For the $f^3, {}^4I_{9/2}$, ground state the coupling constants for the two resulting active Γ_8 levels ($\Gamma_8 \otimes \epsilon_g$ and $\Gamma_8 \otimes \tau_{2g}$ in both cases) are found with use of the numerical data of Lea, Leask, and Wolf,⁶ once the $\langle M_j | \partial V/\partial Q | M_j' \rangle$ matrix elements $\langle {}^9/2 || {}^5/2 \rangle, \langle {}^5/2 || {}^1/2 \rangle, \langle {}^1/2 || -3/2 \rangle, \langle -3/2 || -7/2 \rangle, \langle {}^9/2 || -3/2 \rangle$, and $\langle {}^5/2 || -7/2 \rangle$ have been determined. These elements were therefore calculated from the $f^3, {}^4I_{9/2}, |LSJM_j\rangle$ wave functions, thus yielding sufficient matrix elements both to define all the α, β , and γ quantities and to provide a valuable check on the self-consistency of the results. All the α, β , and γ parameters for the f^1, f^2 , and f^3 systems are listed, together with the $\langle M_j | \partial V/\partial Q | M_j' \rangle$ matrix elements, in the supplementary material. Finally, expressions for the Jahn-Teller coupling constants for the Γ_8 states of $f^3, {}^4I_{9/2}$, are given in Table III

Figure 1. Correlation diagram for f^1 systems in O^* symmetry.Table IV. Calculated Jahn-Teller Stabilization Energies for f^1 Systems in the Weak- and Strong-Field Schemes^a

complex	${}^2F_{5/2}(\Gamma_8)$		${}^2F_{7/2}(\Gamma_8)$		${}^2T_{2u}(\Gamma_8)$		${}^2T_{1u}(\Gamma_8)$		$h\nu$	
	ϵ_g	τ_{2g}	ϵ_g	τ_{2g}	ϵ_g	τ_{2g}	ϵ_g	τ_{2g}	ϵ_g	τ_{2g}
[CeCl ₆] ³⁻	2	4	0	6	0	7	1	4	205	115
[PaF ₆] ²⁻	47	78	2	182	3	74	43	188	310	170
[PaCl ₆] ²⁻	15	19	0	35	1	56	10	29	225	120
[PaBr ₆] ²⁻	14	12	0	15	2	23	5	6	150	83
[PaI ₆] ²⁻	8	7	0	6	2	18	1	1	120	65
[UF ₆] ⁻	115	134	4	324	5	120	99	348	380	185
[UCl ₆] ⁻	55	56	1	107	5	70	38	89	277	136
[UBr ₆] ⁻	47	35	0	47	6	63	20	24	185	90

^a The E_{JT} values listed for the strong-field Γ_8 states are one-fourth of those previously given² for the parent ${}^2T_{1u}$ and ${}^2T_{2u}$ states. All energies are given to the nearest cm^{-1} .

for a range of values of the ratio of the fourth- to sixth-degree potentials in V_{oct} .

For the Jahn-Teller-active levels of T_1, T_2 , and Γ_8 symmetry one should strictly treat couplings of the form $T_{1,2} \otimes (\epsilon_g + \tau_{2g})$ and $\Gamma_8 \otimes (\epsilon_g + \tau_{2g})$, rather than treat the interactions separately, but as previously shown,² the E_{JT} values for f-orbital degeneracies usually prove to be substantially greater for coupling to τ_{2g} than to ϵ_g modes, to some degree justifying this approximation.

Results and Discussion

Figure 1 shows the correlation diagram between the weak- and strong-field schemes for f^1 MX_6 systems in octahedral symmetry, including spin-orbit coupling, while Table IV lists the corresponding values of the Jahn-Teller stabilization energies, E_{JT} , calculated with the assumption of pure weak- or strong-field states, respectively. It is thus clear that the order of magnitude of E_{JT} is not drastically changed between the two approximations, and consequently, since the $|LSJM_j\rangle$ states better reflect the true eigenfunction than do the corresponding strong-field states, it is both more satisfactory and

(9) M. T. Hutchings, *Solid State Phys.*, **16**, 227 (1964).

(10) K. W. H. Stevens, *Proc. Phys. Soc., London, Sect. A*, **65**, 209 (1952).

more convenient to use the former formalism throughout. The only consistent difference for the f^1 species arises in the substantially smaller E_{JT} values for ${}^2F_{7/2}(\Gamma_8) \otimes \epsilon_g$ as compared with those for the correlating system ${}^2T_{1u}(\Gamma_8) \otimes \epsilon_g$ and the generally larger E_{JT} quantities for ${}^2F_{5/2}(\Gamma_8) \otimes \epsilon_g$ as against those for ${}^2T_{2u}(\Gamma_8) \otimes \epsilon_g$. Consequently, for the ${}^2F_{7/2}$ state, the effects produced by trigonal coupling to the τ_{2g} mode (which were already predominant in the strong-field scheme) are now overwhelmingly greater than those due to tetragonal coupling to the ϵ_g mode. For the ${}^2F_{5/2}$ state the E_{JT} values for ϵ_g and τ_{2g} coupling are now clearly comparable, whereas for the strong-field ${}^2T_{2u}(\Gamma_8)$ state coupling to the τ_{2g} mode predominated.

In either case however the E_{JT} values calculated from the linear adiabatic coupling constants show that for most species the resulting Jahn–Teller coupling will be relatively weak since the ratio $E_{JT}/h\nu$ only twice exceeds unity and is usually well below that value. Moreover, the same result proves also to be true for the f^2 and f^3 systems studied here (vide infra), so that in general Jahn–Teller effects for f^x species should be essentially dynamic in character. For such a situation, $E_{JT} < h\nu$ (or $\ll h\nu$), the anticipated behavior will depend upon whether the Jahn–Teller-active level constitutes the ground state or some excited state of the system considered: in the latter case it should still in principle be possible, for transitions to such levels, to observe splittings (related to E_{JT}) of Jahn–Teller origin, but for the former no such direct manifestation would be expected. In addition, the lanthanide and actinide species show spin–orbit coupling constants, ξ , well in excess of the predicted E_{JT} quantities so that, with $\xi > h\nu > E_{JT}$, indirect contributions such as the Ham effect should also be relatively small.

The f^1 , f^2 , and f^3 MX_6 species of the $4f$ and $5f$ series for which the data needed to calculate E_{JT} are available are limited to the trivalent lanthanide systems $[\text{Ln}^{\text{III}}\text{Hal}_6]^{3-}$ and the tetravalent and pentavalent actinide complexes $[\text{An}^{\text{IV}}\text{Hal}_6]^{2-}$ and $[\text{An}^{\text{V}}\text{Hal}_6]^-$. However, the data for the elpasolite lanthanide $\text{Cs}_2\text{NaLnCl}_6$ systems must be interpreted with some care since, for the lighter lanthanides at least, a low-temperature phase transition occurs between room temperature and 77 K, resulting in a distortion of the perfect cubic symmetry of the O_h^5 space group found at room temperature and a lowering of the O_h point symmetry about the individual Ln atoms.

Thus single-crystal magnetization and NMR measurements¹¹ show that the lighter $\text{Cs}_2\text{NaLnCl}_6$ salts (Ce, Nd), unlike the heavier members (e.g., Ho), are tetragonally distorted at lower temperatures, the Γ_8 ground level of the f^3 Nd^{III} system being split into two doublets almost 2 K apart. For the Pr^{III} salt electronic Raman studies¹² indicate that the distortion is established on cooling to about 70 K, while MCD and absorption spectra measurements¹³ confirm that for $\text{Cs}_2\text{NaPrCl}_6$ a lowering of the cubic symmetry takes place between room temperature and 77 K. The transition temperature was found¹⁴ to be 158 K for Pr^{III} and 138 K for Nd^{III} . Studies of the ESR spectra of Gd^{III} in various $\text{Cs}_2\text{NaLnCl}_6$ hosts¹⁵ indicated a similar effect, and the distortion was attributed to a marginal structural misfit between the Ln^{3+} ions and the elpasolite lattice. It was inferred that similar phase transitions should occur for the lighter lanthanides as far as Eu; the position of Gd was unclear, but Tb was predicted to be resistant to distortion.

Table V. Ligand Field Parameters and Calculated Jahn–Teller Stabilization Energies for Components of the ${}^3\text{H}_4$ Ground States of f^2 Systems^a

	$4f^2$		$5f^2$
	$[\text{PrF}_6]^{3-}$ ^b	$[\text{PrCl}_6]^{3-}$ ^c	$[\text{UCl}_6]^{2-}$ ^d
B_0^4 , cm^{-1}	3920	2175	7296
B_0^6 , cm^{-1}	480	269	904
e_σ , cm^{-1}	775	431	1445
e_π , cm^{-1}	287	158	530
$\partial e_\sigma/\partial R$, 10^{11} cm^{-2}	-1.67	-0.79	-2.74
$\partial e_\pi/\partial R$, 10^{11} cm^{-2}	-0.44	-0.21	-0.72
R , Å	2.38	2.83	2.72
K_e , mdyn Å^{-1}	1.17	0.70	1.2
K_T , mdyn Å^{-1}	0.03	0.02	0.05
$E_{JT}(\Gamma_3(E) \otimes \epsilon_g)$, cm^{-1}	5	2	13
$E_{JT}(\Gamma_4(T_1) \otimes \epsilon_g)$, cm^{-1}	7	3	19
$E_{JT}(\Gamma_4(T_2) \otimes \epsilon_g)$, cm^{-1}	2	1	6
$E_{JT}(\Gamma_4(T_1) \otimes \tau_{2g})$, cm^{-1}	9	3	14
$E_{JT}(\Gamma_4(T_2) \otimes \tau_{2g})$, cm^{-1}	55	18	89
$h\nu(\epsilon_g)$, cm^{-1}	335	205	225
$h\nu(\tau_{2g})$, cm^{-1}	170	115	120

^a Data from sources cited in ref 2 and from references listed below. ^b Reference 17. ^c Reference 12. ^d Reference 18.

For the Cs_2MLnF_6 complexes ($M = \text{Na}, \text{K}$) cubic O_h^5 space groups were again reported,¹⁶ but there is no information as to whether or not phase transitions may occur at lower temperatures. However, there is definite evidence (vide infra) for such transitions in $[\text{U}^{\text{IV}}\text{Cl}_6]^{2-}$ and $[\text{U}^{\text{III}}\text{Cl}_6]^{3-}$, while the $[\text{An}^{\text{V}}\text{Hal}_6]^-$ anions are already known to be distorted from perfect cubic symmetry even at room temperature. However, the occurrence of low-temperature distortions from cubic symmetry is itself clearly unlikely to be of Jahn–Teller origin since the distorted structure often persists to relatively high temperatures, and its manifestation is independent of the ground state of the light lanthanide (or actinide) concerned; in $\text{Ce}^{\text{III}}(\Gamma_7)$ and in Pr^{III} and U^{IV} (both Γ_1) the O^* ground states are indeed Jahn–Teller impotent. Nevertheless, at least for the $[\text{LnCl}_6]^{3-}$ species, the distortions appear to lead to splitting of erstwhile degenerate levels of only a few cm^{-1} , so that there may well arise situations in which the distortion splitting, Δ , and E_{JT} are of comparable magnitude; this condition, $\Delta \approx E_{JT}$, further complicates any detailed theoretical treatment of these systems, but Jahn–Teller activity should not be totally quenched unless $\Delta \gg E_{JT}$.

f^1 Systems. The $4f^1$ compound $\text{Cs}_2\text{NaCeCl}_6$ needs little extra comment: no splitting is found in the electronic Raman spectrum for the upper (mainly ${}^2F_{7/2}$) Γ_8 level, and the 15-cm^{-1} separation in the lower (mainly ${}^2F_{5/2}$) Γ_8 level could be due simply to the lattice distortion. However, since the gap between the Jahn–Teller potential sheets should be $4E_{JT}$, Jahn–Teller contributions cannot be entirely discounted. The $5f^1$ $[\text{Pa}^{\text{IV}}\text{Hal}_6]^{2-}$ and $[\text{U}^{\text{V}}\text{Hal}_6]^-$ species again require little further discussion. Thus, although by analogy with the $[\text{U}^{\text{IV}}\text{Cl}_6]^{2-}$ anion (vide infra) it is possible that the $[\text{Pa}^{\text{IV}}\text{Hal}_6]^{2-}$ systems also undergo phase transitions at lower temperatures, no fundamental change in their electronic spectra with temperature was reported. Moreover, while lattice distortions in these systems should not yield splittings very much larger than for the Ln^{III} complexes, the magnitudes of the e_λ parameters suggest that any Jahn–Teller effects should be appreciably larger for An^{IV} than for Ln^{III} compounds. Consequently, the attribution² of the substantial splittings of the upper Γ_8 levels in the electronic spectra of the $[\text{PaHal}_6]^{2-}$ complexes to Jahn–Teller effects appears to be reasonably soundly based. Similarly, although the $[\text{U}^{\text{V}}\text{Hal}_6]^-$ anions previously discussed² did not show perfect cubic symmetry, the splittings of the upper Γ_8 level were, as required by the e_λ values, significantly greater

- (11) R. Nevald, F. W. Voss, O. V. Nielson, H.-D. Amberger, and R. D. Fischer, *Solid State Commun.*, **32**, 1223 (1979).
 (12) H.-D. Amberger, *Z. Anorg. Allg. Chem.*, **439**, 48 (1978).
 (13) R. W. Schwartz, *Mol. Phys.*, **31**, 1909 (1976).
 (14) A. T. Anistratov, B. V. Bexnosikov, and V. A. Gusar, *Sov. Phys.—Solid State (Engl. Transl.)*, **20**, 2138 (1978).
 (15) R. W. Schwartz, S. F. Watkins, C. J. O'Connor, and R. L. Carlin, *J. Chem. Soc., Faraday Trans. 2*, **72**, 565 (1976).

- (16) I. Siddiqi and R. Hoppe, *Z. Anorg. Allg. Chem.*, **374**, 225 (1970).

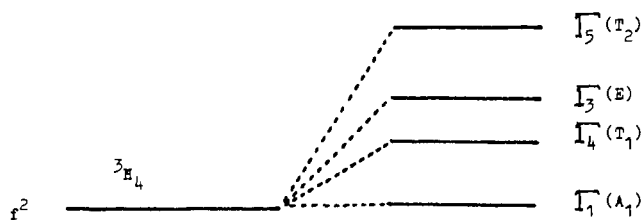


Figure 2. Splitting diagram for f^2 , 3H_4 , systems in O^* symmetry.

than for the $[Pa^{IV}Hal_6]^{2-}$ systems and too great to be ascribed to relatively small departures from O_h symmetry. The weak-field E_{JT} values are therefore simply given in Table IV without additional comment.

f^2 Systems. In Table V the calculated E_{JT} values for some f^2 systems are listed, and for the $4f^2$ complex $Cs_2NaPrCl_6$, the results clearly indicate that the coupling 3H_4 (Γ_3) \otimes τ_{2g} should lead to much larger splittings than for any of the other 3H_4 components coupling to either active mode. Paradoxically however, it seems that of the transitions from the inactive Γ_1 ground level to the degenerate Γ_3 , Γ_4 , and Γ_5 components of 3H_4 (see Figure 2) only that to the Γ_5 level shows no splitting in the electronic Raman spectrum.¹² The Γ_3 and Γ_4 levels do show small splittings of 10 and 14 cm^{-1} , respectively, and these could be due simply to low-symmetry distortions, although it is then difficult to see why the Γ_5 level remains unsplit. In contrast, for the hexafluoro system Cs_2KPrF_6 , the transition to the Γ_5 level shows¹⁷ a substantial splitting of just over 100 cm^{-1} in the electronic Raman spectrum, but strangely, although the Γ_3 level displays a small separation of 13 cm^{-1} , the Γ_4 level was found to be unsplit. Further study of these $4f^2$ systems therefore appears necessary before the experimental results can be rationalized.

Moreover, the results for the $5f^2$ anion $[UCl_6]^{2-}$ also pose some problems. Thus the splitting of the 3H_4 ground manifold in O^* symmetry has been directly observed in the electronic Raman spectrum only for the Cs_2UCl_6 salt,¹⁸ and although the $[UCl_6]^{2-}$ unit in this complex deviates only marginally from strict cubic symmetry, Cs_2UCl_6 exhibits a D_{3d}^3 space group,¹⁹ rather than the O_h^5 symmetry found²⁰ for the tetramethylammonium compound $(NMe_4)_2UCl_6$. In the low-temperature Raman spectrum electronic peaks, corresponding to transitions from the Γ_1 ground component to the Γ_3 and Γ_4 levels of 3H_4 , are observed, these being split by 73 and 125 cm^{-1} , respectively. These splittings could be due merely to low-symmetry distortions, although they are compatible with the calculated E_{JT} values of Table V, but the electronic Raman spectrum at the frequency anticipated for the $\Gamma_1 \rightarrow \Gamma_5$ transition (for which the largest E_{JT} is calculated) is obscured by fluorescence. However, it has been shown²¹ that even $(NMe_4)_2UCl_6$, which appears to be strictly cubic at room temperature, undergoes a phase transition to lower symmetry between 131 and 116 K, and a study of the electronic Raman transition 3H_4 (Γ_1) \rightarrow 3H_4 (Γ_4) shows that this peak is split into two components below the transition temperature but appears as a single band above that point. Consequently it is again difficult to disentangle any possible Jahn-Teller effects from those due to low-symmetry distortions.

f^3 Systems. The f^3 system in O^* symmetry is the first of the f^x species showing a Jahn-Teller-active (Γ_8) ground state, and in the $4f^3$ compound $Cs_2NaNdCl_6$, the electronic Raman spectrum²² identified two transitions within the ${}^4I_{9/2}$ manifold,

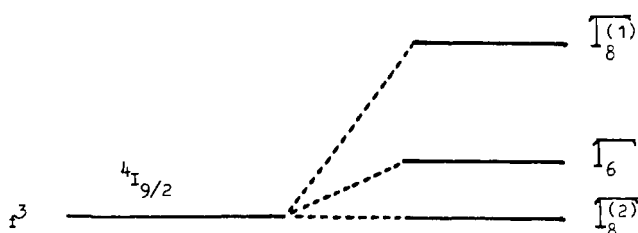


Figure 3. Splitting diagram for f^3 , ${}^4I_{9/2}$, systems in O^* symmetry.

Table VI. Ligand Field Parameters and Calculated Jahn-Teller Stabilization Energies for Components of the ${}^4I_{9/2}$ Ground State of f^3 Systems^a

	$[NdCl_6]^{3-}$ ^b	$[NpCl_6]^{2-}$ ^c	$[NpCl_6]^{2-d}$
B_0^4 , cm^{-1}	1792	4160	6000
B_0^6 , cm^{-1}	286	2413	720
e_σ , cm^{-1}	363	1071	1185
e_π , cm^{-1}	105	-441	445
$\partial e_\sigma / \partial R$, $10^{11} cm^{-2}$	-0.68	-2.22	-2.26
$\partial e_\pi / \partial R$, $10^{11} cm^{-2}$	-0.11	+1.52	-0.62
R , Å	2.80	2.70	2.70
K_ϵ , $mdyn \text{ \AA}^{-1}$	0.70	1.20	1.20
K_τ , $mdyn \text{ \AA}^{-1}$	0.02	0.05	0.05
$E_{JT}(\Gamma_8^{(1)} \otimes \epsilon_g)$, cm^{-1}	0.4-0.5 ^e	24-25	1.6-1.7
$E_{JT}(\Gamma_8^{(2)} \otimes \epsilon_g)$, cm^{-1}	0	3.5-3.1	0.1
$E_{JT}(\Gamma_8^{(1)} \otimes \tau_{2g})$, cm^{-1}	4.4-5.6	177-235	10-13
$E_{JT}(\Gamma_8^{(2)} \otimes \tau_{2g})$, cm^{-1}	0.8-1.3	35-37	1.7-2.8
$h\nu(\epsilon_g)$, cm^{-1}	205	225	225
$h\nu(\tau_{2g})$, cm^{-1}	115	120	120

^a Data from sources cited in ref 2 and from references listed below. ^b Reference 22. ^c Reference 26. ^d Estimated from Pa^{IV} and U^{IV} data together with known trends in the 5f series. ^e All E_{JT} values are listed for the parameter range $x = 0.4-0.8$; see ref 6 and Table III. The ground component is $\Gamma_8^{(2)}$.

from the ground component Γ_8 level to Γ_6 and Γ_8 states, respectively (see Figure 3). The calculated Jahn-Teller stabilization energies for $[NdCl_6]^{3-}$ are included in Table VI, E_{JT} values for the more effective τ_{2g} coupling of about 1 and 5 cm^{-1} being predicted for the lower and upper Γ_8 levels, respectively (in the nomenclature of Lea, Leask, and Wolf⁶ the ground level is $\Gamma_8^{(2)}$ and the excited state $\Gamma_8^{(1)}$). For this Nd^{III} salt a discontinuity at about 15 K in the plot of the inverse susceptibility, χ^{-1} , against T suggests a splitting of the ground-state Γ_8 level of some 10 cm^{-1} , which is rather greater than the 1-2 cm^{-1} indicated by the magnetization and NMR results, but since the calculated E_{JT} values for $\Gamma_8^{(2)}$ are much smaller than the zero-point energies of the active vibrational modes ($E_{JT} \ll h\nu$), no observable ground-state splitting should result from Jahn-Teller activity. The observed splitting,^{11,22} which is either comparable to or greater than E_{JT} , must therefore be attributed to low-symmetry distortions, and it would be necessary to search for small indirect consequences (such as the Ham effect) to provide evidence of Jahn-Teller activity. For the excited $\Gamma_8^{(1)}$ level somewhat larger E_{JT} values are predicted, which might lead to observable splittings, but the electronic peaks in the Raman spectrum are rather weak, and no separation of the $\Gamma_8^{(1)}$ level was detected.

For the 5f³ configuration some data are available for both the $[U^{III}Cl_6]^{3-}$ and the $[Np^{IV}Cl_6]^{2-}$ anions. For Cs_2NaUCl_6 the low-temperature magnetic susceptibility indicated²³ a magnetic moment of 2.92 μ_B above about 20 K, in good agreement with the value predicted for a Γ_8 ground state, falling to 2.49 μ_B below that temperature. There are unfortunately no spectroscopic results from which the e_λ for this

(17) H.-D. Amberger, *Inorg. Nucl. Chem. Lett.*, **14**, 491 (1978).

(18) H.-D. Amberger, R. D. Fischer, G. G. Rosenbauer, and A. W. Spiegl, *Ber. Bunsenges. Phys. Chem.*, **80**, 495 (1976).

(19) S. Siegl, *Acta Crystallogr.*, **9**, 827 (1956).

(20) E. Staritzky and J. Singer, *Acta Crystallogr.*, **5**, 536 (1952).

(21) W. Von der Ohe, *J. Chem. Phys.*, **63**, 2949 (1975).

(22) H.-D. Amberger, G. G. Rosenbauer, and R. D. Fischer, *J. Phys. Chem. Solids*, **38**, 379 (1977).

(23) M. E. Hendricks, E. R. Jones, J. A. Stone, and D. G. Karraker, *J. Chem. Phys.*, **60**, 2095 (1974).

complex might be determined, but even were these substantially greater than for the 4f series, one would still predict $E_{JT} < h\nu$. Consequently no observable Jahn–Teller splitting would be anticipated, so that the break in the χ^{-1} vs. T plot at 20 K must result from a low-symmetry distortion which splits the $\Gamma_8^{(2)}$ ground level by about 13 cm^{-1} .

For $[\text{NpCl}_6]^{2-}$ there is again difficulty in defining the e_λ parameters. Thus for Cs_2NpCl_6 weak bands at 900 and 966 cm^{-1} in the 77 K absorption spectrum²⁴ were attributed to transitions within the $^4I_{9/2}$ manifold from the Γ_8 ground level to excited Γ_6 and Γ_8 levels, respectively; this assumption, together with an analysis of the limited part of the $5f^3$ energy levels below $13\,000 \text{ cm}^{-1}$, was then used to derive the B_0^4 and B_0^6 crystal field quantities, from which the e_λ may be derived. However, for $[\text{PaCl}_6]^{2-}$ and $[\text{UCl}_6]^{2-}$ e_σ and e_π respectively are both of quite comparable magnitude (see Tables IV and V), with e_π/e_σ equal to 0.52 for Pa and 0.37 for U, but for $[\text{NpCl}_6]^{2-}$ the B_k^q 's lead to a somewhat smaller e_σ and a negative e_π (see Table VI). The former result is a reasonable consequence of the actinide contraction, but a negative e_π would, improbably, require the ligand 3p π orbitals to be at higher energies than the metal 5f levels, thereby rendering the reported B_k^q values inherently suspect.

In Table VI therefore the E_{JT} values are calculated for $[\text{NpCl}_6]^{2-}$ both for the experimentally derived²⁴ e_λ and for e_λ values deduced by analogy with the Pa^{IV} and U^{IV} complexes. The former yield a value of $35\text{--}55 \text{ cm}^{-1}$ for $\Gamma_8^{(2)} \otimes \tau_{2g}$ (e_g coupling gives a smaller E_{JT}) and the latter only some 2 cm^{-1} for the same coupling. However, since the e_σ and e_π contributions to the A constants are of opposite sign, E_{JT} is clearly highly sensitive to the relative magnitudes and the respective signs of e_σ and e_π , although within the constraints of the calculation the two sets of results probably afford reasonable bounds for E_{JT} .

Thus the situation for $[\text{NpCl}_6]^{2-}$ is again $E_{JT} < h\nu$ (or $\ll h\nu$) and the available magnetic susceptibility data afford only rather equivocal evidence for indirect manifestations of Jahn–Teller activity. Thus Stone and Karraker²⁵ reported the low-temperature χ^{-1} vs. T behavior for the Cs, NMe_4 , and NEt_4 salts, but of these only $(\text{NMe}_4)_2\text{NpCl}_6$ is strictly cubic (O_h^2), the Cs and NEt_4 compounds showing slightly distorted structures of trigonal (D_{3d}^3) and orthorhombic (D_{2h}^2) symmetry, respectively.^{19,20} For the Cs and NEt_4 salts the plots of χ^{-1} vs. T are linear at the very lowest temperatures but above 7 and 15 K respectively show marked curvature before linearity

is resumed above 50 and 56 K. The effective magnetic moments, μ , are 1.80 and $1.86 \mu_B$ in the low-temperature region and 3.07 and $3.10 \mu_B$ at higher temperatures, the latter agreeing well with the magnetic moment calculated^{24,26} for the Γ_8 ground level of such an f^3 system. Moreover, an effective μ value of around $2.0 \mu_B$ is expected²⁷ for a trigonally distorted system, in good agreement with the results for the lowest temperature, so that it is reasonable to conclude that the discontinuities in the χ^{-1} vs. T plots for the Cs and NEt_4 salts reflect a low-symmetry distortion which splits the Γ_8 ground level by some $15\text{--}30 \text{ cm}^{-1}$. On the other hand, for $(\text{NMe}_4)_2\text{NpCl}_6$, which, at least at room temperature, shows the strictly cubic O_h^2 space group, the χ^{-1} vs. T plot shows no break between 2.5 and 50 K. This is obviously consistent with the undistorted O_h structure, but the magnetic moment of only $2.10 \mu_B$ is well below the result (ca. $3.0 \mu_B$) expected for the Γ_8 ground level. It is possible that a Jahn–Teller reduction of the magnitudes of certain electronic operators may play a part in this result, but further investigation of this unexplained observation is clearly needed.

Conclusions

For many of the f^x systems here treated E_{JT} proves to be substantially smaller than $h\nu$, and frequently $E_{JT}/h\nu$ is as little as 0.1 or less. Experimental indications of Jahn–Teller effects of this order of magnitude will therefore be difficult to obtain, but such evidence has been adduced in a number of cases—see Englman²⁷ for a listing thereof. Nevertheless, further discussion of the manifestation of the Jahn–Teller effect in these systems and of its possible interaction with existing distortions from perfect octahedral symmetry lies beyond the scope of this study. The most frequently occurring situation, $\xi > h\nu > E_{JT} \approx \Delta$ (or $< \Delta$), clearly requires further theoretical work, especially on possible reductions of electronic magnitudes by Jahn–Teller activity, while additional experimental information is needed relating to magnetic susceptibilities, ESR investigations, and electronic spectra, especially the measurement of the electronic Raman spectrum within the $5f^3$, $^4I_{9/2}$, manifold.

Registry No. $[\text{CeCl}_6]^{3-}$, 27796-27-6; $[\text{PaF}_6]^{2-}$, 49864-66-6; $[\text{PaCl}_6]^{2-}$, 44463-14-1; $[\text{PaBr}_6]^{2-}$, 44463-09-4; $[\text{PaI}_6]^{2-}$, 44463-23-2; $[\text{UF}_6]^-$, 48021-45-0; $[\text{UCl}_6]^-$, 44491-58-9; $[\text{UBr}_6]^-$, 44491-06-7.

Supplementary Material Available: Tables of one-electron $\partial V/\partial Q$ matrix elements in the real and complex f -orbital basis and of $\langle M_j \partial V/\partial Q | M_j' \rangle$ matrix elements for f^1 , f^2 , and f^3 systems (12 pages). Ordering information is given on any current masthead page.

(24) E. R. Menzel and J. B. Gruber, *J. Chem. Phys.*, **54**, 3857 (1971).
 (25) J. A. Stone and D. G. Karraker, Report DP-MS-71-86, E. I. du Pont de Nemours and Co., Aiken, SC 29801, 1972.

(26) J. B. Gruber and E. R. Menzel, *J. Chem. Phys.*, **50**, 3772 (1969).
 (27) R. Englman, "The Jahn–Teller Effect in Molecules and Crystals", Wiley-Interscience, New York, 1972.